

A recyclable epoxy for composite wind turbine blades

Ming-Sung Wu, Bo Cheng Jin, Xin Li & Steven Nutt

To cite this article: Ming-Sung Wu, Bo Cheng Jin, Xin Li & Steven Nutt (2019) A recyclable epoxy for composite wind turbine blades, *Advanced Manufacturing: Polymer & Composites Science*, 5:3, 114-127, DOI: [10.1080/20550340.2019.1639967](https://doi.org/10.1080/20550340.2019.1639967)

To link to this article: <https://doi.org/10.1080/20550340.2019.1639967>



© 2019 The Author(s). Published by Informa UK Limited, trading as Taylor & Francis Group



Published online: 10 Jul 2019.



Submit your article to this journal [↗](#)



Article views: 1746



View related articles [↗](#)



View Crossmark data [↗](#)



Citing articles: 1 View citing articles [↗](#)



A recyclable epoxy for composite wind turbine blades

Ming-Sung Wu^a , Bo Cheng Jin^b, Xin Li^c and Steven Nutt^a

^aDepartment of Chemical Engineering and Materials Science, University of Southern California, Los Angeles, CA, USA;

^bDepartment of Aerospace and Mechanical Engineering, University of Southern California, Los Angeles, CA, USA; ^cAdesso Advanced Materials UK Co. Ltd., St. John's Innovation Centre, Cambridge, UK

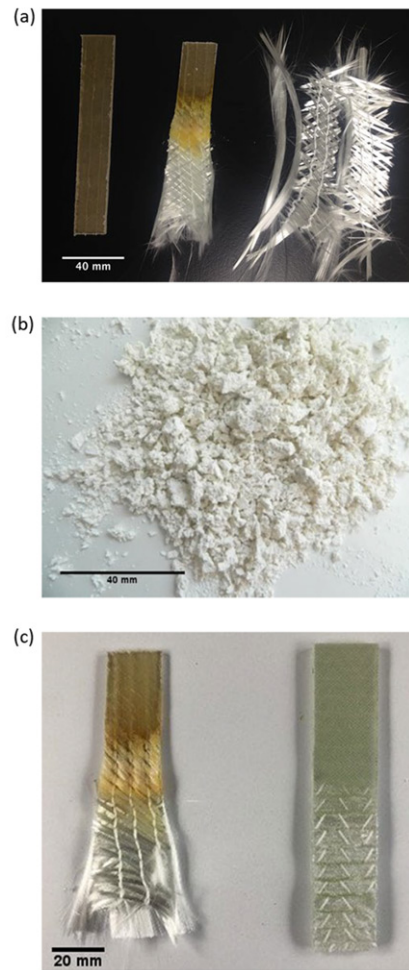
ABSTRACT

Disposal of wind turbine blades, which are generally non-biodegradable and non-recyclable products comprised largely of fiber-reinforced thermoset polymers (FRPs), pose environmental problems when components reach end-of-service-life. Because the global wind turbine market shows steady year-over-year growth, the need for a recycling solution for wind blade FRPs is urgent and growing rapidly. In the present study, recyclable resins, formulated using proprietary epoxy curing agents (Cleavamine[®], Adesso), were characterized and analyzed for processability and recyclability. Protocols for vacuum infusion processing were developed for these recyclable resins. Secondly, laminates of glass fibers and the above epoxy matrices were first produced then recycled, and the properties of recovered fibers were evaluated. Matrix and laminate properties were compared to a benchmark commercial epoxy presently used in commercial wind blades. Results showed that vacuum infusion with the recyclable resins yielded laminates with low void contents and properties comparable to non-recyclable commercial epoxies, and the recovered glass fibers retained surface quality comparable to virgin fibers. Furthermore, results also showed that the recovered matrix residue can be re-used in second-life applications, effectively completing the closed-loop recycling method in this study.

KEYWORDS

Recycling; processing; epoxy; glass fiber; thermoset; composites; mechanical properties; vacuum infusion; dissolution

GRAPHICAL ABSTRACT



The graphic abstract figure provides a general idea for (a) Recovered glass fibers after Acid-digestion treatment, (b) reclaimed resin powder after recycling and (c) recyclability comparison with other commercial epoxy system.

1. Introduction

Wind energy has grown rapidly over the past two decades. In fact, the overall capacity of all wind turbines installed worldwide by the end of 2017 reached 539,291 megawatts, according to preliminary statistics published by World Wind Energy Association (WWEA) [1]. In 2017 alone, 52,552 megawatt was added, slightly more than in 2016, when 51,402 megawatts went online [1]. The market growth is expected to continue. In addition, since the 1980s, the sizes of wind turbine blade sizes have increased eight-fold, surpassing 100 meters in length, harvesting green energy to meet global demand [2]. The demand for longer blades is being addressed by the development of lighter structures, particularly those based on fiber-reinforced polymers (FRPs). The projected lifespan of these wind blades is roughly 20–25 years, and presently, the only option for disposal at end-of-blade-life is to

landfill. Thus, within the next 25 years, 225,000 tons per year of FRP-based rotor blades worldwide are projected to reach the end of life and require disposal, or preferably, recycling [3]. To prevent waste and recover economic and environmental value, the wind energy sector requires more efficient materials and processing, more reliable performance, and FRPs that are recyclable. The focus of this work is the development of processes for such FRPs, which offer major economic and environmental benefits.

Recent reports have described the state of the art for reuse and recycling of composite materials [4–17]. Recycling of thermoset composites (particularly epoxies) presents a challenge due to their highly cross-linked structures and insolubility under mild conditions [18, 19]. While landfills remain the least expensive option for end-of-life disposal, most European Union (EU) member states have passed laws in the past decade forbidding landfill disposal

of composites [20]. In the same time period, multiple technologies have been developed to explore the feasibility of recycling FRPs. Currently, there are two physical recycling approaches practiced on industrial scales: mechanical grinding [21–27] and pyrolysis (including other thermal processes [28–33]). The main advantage of physical recycling methods is that composite materials comprised of different matrix polymers and fiber reinforcements can be accommodated by a single process, although the matrix generally cannot be recovered. Also, long clean fibers cannot be recovered after mechanical grinding, limiting second-use applications. Pyrolysis (thermal processing) is the most widely practiced recycling process, and it is used extensively for industrial scale recycling. However, pyrolysis destroys polymer matrices, and fibers are often degraded due to high-temperature treatment. Fibers recovered from thermal processing are generally chopped into short lengths for use in molding compounds, and most of the value of the continuous fibers is lost. Due to the limited market demand for recycled short fibers, most composites are not being recycled today.

To overcome the limitations of grinding and pyrolysis, lab-scale chemical processes have been developed to recover clean fibers (99.9% purity) with greater than 90% strength retention [34]. For example, supercritical fluids have received attention because of the ability to tailor the operating conditions (temperature, pressure, and volume) for specific composites. However, the severity of the conditions and the high cost of the associated equipment have limited development. Also, because of the batch nature of the process, scaling presents challenges. Recent investigations have considered less severe conditions, although the process times increase markedly [35–37]. The toxicity of solvents and/or catalysts, as well as the damage to fibers and severity of process conditions have limited present attempts to recycle FRPs.

So far, recycling of FRPs by chemical degradation has received only limited consideration, and chemical recycling methods have not been employed on an industrial-scale recycling due to a few conundrums. First, the high capital costs typically required to achieve high temperature and pressure, as well as the batch nature of the process, are incompatible with large-scale deployment. Second, the solvent and/or catalysts toxicity issues must be solved before large-scale usage. Finally, the post-treatment methods for chemical solutions after recycling are not yet mature. Most chemical recycling methods have focused on amine-cured bisphenol A type epoxies (bi-functional epoxy) [38–40], which feature relatively low crosslink density and glass transition

temperature (T_g). For example, both depolymerization (benzyl alcohol/ K_3PO_4 at 200 °C) and acid digestion (acetic acid/ H_2O_2 at 110 °C) were shown to be effective for amine-cured neat epoxy with high crosslink density [41–43]. In contrast, the present work attempts to demonstrate more effective chemical treatments for amine/epoxy composites recycling that can be performed under moderate conditions, i.e. atmospheric pressure, moderate temperature condition (80 °C and 110 °C), and a relatively mild acid [44]. Catalyst usage is avoided to simplify the recycling procedure, limit cost and ensure safety.

If and when such a process is deployed on a large scale for treatment of retired wind blades, the process will yield large quantities of (mostly) continuous glass and carbon fibers, as well as feedstocks for recycled polymers [45–47]. Overall, the ability to recycle the end-of-life wind blades will provide a much-needed increase in the sustainability of the energy industry. The most expedient use of recovered fibers may be as fillers in molding compounds [21, 22, 48–50]. However, industrial applications using recycled fibers or resins are presently rare, and there is little market “pull” for such products, resulting in an oversupply of recovered fibers. The situation stems from multiple factors, including (1) performance/cost ratio relative to virgin glass fibers, (2) fiber surface quality (sizings are typically removed by digestion solutions), and (3) recovered fibers lack uniformity in terms of length distribution and organization. Thus, reaching sustainability of FRPs requires both advances in the separation technology (to make recycling feasible on a large scale), as well as development of markets and applications for the recovered products.

A recyclable epoxy resin was formulated based on a cleavable curing agent (Adesso Cleavamine) [51–53]. The cured epoxy can be chemically separated from fiber reinforcements and subsequently recycled under moderate pressure and temperature to yield small polymer molecules/segments. Thermochemical and thermomechanical properties of a prototype resin system were evaluated to determine in-process cure kinetics and viscosity profile. A vacuum infusion (VI) process was demonstrated to produce lab-scale FRP panels, from which the mechanical properties were measured. The fibers and matrix of prototype laminates were subsequently separated using an aqueous-organic mixture, and the properties of the reclaimed fibers were documented. The study demonstrates a viable pathway for large-scale recycling of FRPs based on an epoxy formulation yielding performance comparable to those presently used in large-scale production of wind turbine blades.

2. Experiments

2.1. Resin formulation

The recyclable resin selected (rAFV-1005G2, Adesso) was a two-component (mixing ratio of 100:18.6, parts by weight), low-viscosity epoxy designed for vacuum infusion. By design, the curing agents contained acid-labile formyl, and acetal or ketal bonds in the molecule. Fiber-reinforced composite parts produced from epoxy resins cured with a matched curing agent (Cleavamine®) can be dissolved in an aqueous-organic solvent mixture under mild conditions, i.e. at atmospheric pressure and $T < 110^{\circ}\text{C}$.

The acetal or ketal linkage in the curing agents can be cleaved by acid hydrolysis during the dissolution process to yield useful molecular products. In the development of recyclable rAFV-1005G2 resin for vacuum infusion processes, the curing agents (Cleavamine®, Figure 1) were selected to yield T_g , gel time, viscosity, and processing characteristics suitable for wind turbine blades and FRP recycling [51, 53].

In tests for recycling the reclaimed resin, different weight percentages (by mass) of reclaimed resin powder (5 wt%, 10 wt% and 20 wt%) first were blended with neat resin using a mixing ratio of recycle-to-curing agent of 100:18.6. The blend ratio yielded a homogeneous mixture, a requisite before proceeding with the subsequent vacuum infusion process.

2.2. Thermal analysis

TGA experiments were performed to determine the degradation temperature of epoxy samples by measuring weight loss as a function of temperature. In each TGA test, samples were heated from 30 to 350°C at a rate of $1.5^{\circ}\text{C}/\text{minute}$. From the TGA data, the polymer degradation temperature, defined as the temperature at which 5% sample weight loss occurred, was determined ($T_d = 280.4^{\circ}\text{C}$). The measured T_d set an upper limit for further calorimetric tests.

The cure kinetics of the resin were determined using modulated differential scanning calorimetry (MDSC), employing both isothermal and dynamic measurements (TA Instruments Q2000 DSC, New Castle, DE). MDSC yields accurate heat capacity measurements with a single experiment and allows separation of the total heat flow into reversing and nonreversing heat flow components [54–57]. Both isothermal and dynamic measurements were performed to measure the degree of cure (DoC).

The MDSC measurements were performed under a constant flow of nitrogen (50 mL/min). Prior to each DSC scan, the uncured sample (7–20 mg) was sealed in a pan, placed in the DSC cell, and pre-cooled to -40°C . For dynamic MDSC measurements, the DSC cell was subsequently heated at a rate of 1, 2, 5 and $10^{\circ}\text{C}/\text{minute}$ from -40 to 250°C with $\pm 0.5^{\circ}\text{C}/\text{minute}$ modulation. For isothermal measurements, the objective was to determine the relationship between the DoC and the glass transition temperature (T_g). Three isothermal cure temperatures were selected (60 , 80 and 100°C) between the onset of the reaction and the peak heat flow from the dynamic scan. In these isothermal tests, the DSC cell was heated to the cure temperature, then held at that temperature for times ranging from 2 min to 2 h. Table 1 lists the temperatures and hold-times used to reach specific cure states. Following scans, the DSC cell was cooled to -40°C , then heated to 250°C at $10^{\circ}\text{C}/\text{min}$ to measure the residual heat of reaction (ΔH_R). The T_g value was determined from the inflection point of the step-wise transition.

2.3. Rheometry

Viscosity (η) measurements were conducted using a rheometer (TA Instruments AR2000) with

Table 1. Parameters of MDSC tests.

Curing temperature T_c ($^{\circ}\text{C}$)	Hold times t_h (min)
60	15, 40, 60, 120, 240, 300
80	15, 40, 60, 120, 240, 300
100	1, 5, 15, 20, 40, 60, 120, 240, 300

Note: Vitrification was observed during isothermal curing.

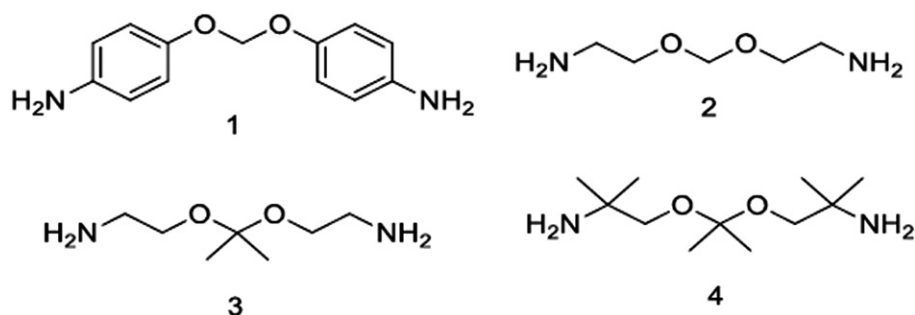


Figure 1. Cleavamine® curing agents applied in this work.

aluminum parallel plates. All tests were performed under constant oscillatory shear at a frequency of 1 Hz and at a strain value of 0.25%, within the linear viscoelastic (LVE) regime of all resin systems. The resin samples were sandwiched between the plates and compressed to a gap of 0.5 mm. Nonisothermal cures were conducted by heating at 2.0 °C/min from 20 to 250 °C, and isothermal dwells were performed by heating at 10 °C/min to 60, 80 and 100 °C to determine the gel-time and viscosity profile. The stop condition was set as 90% of maximum torque (200 mN•m) in both nonisothermal and isothermal tests.

2.4. Composite fabrication

Stitched unidirectional E-glass fiber was selected as the reinforcement (non-crimp fabric, NCF, 955 g/m², Fibre Glast Developments Corp[®]). NCF glass was chosen because of affordability, superior drapability, and ability to conform to curved surfaces typical of wind blades. Fiber sheets 250 × 250 mm² were cut and stacked to form two-layer, four-layer, and eight-layer preforms. The infusion area was prepared by removing dust, and the tool surface was treated with a mold release agent prior to infusion. Cut plies were placed on a Teflon film, creating the preform, and a peel ply (ECONOSTITCH, *Airtech International*) was placed over the preform. To ensure even resin distribution through the preform, a spiral slit hose was used at the inlet and outlet of the cavity, cut to a length of 260 mm and placed at the edge of the fiber sheets. Distribution media (Greenflow 75, *Airtech*) were laid over the peel ply to enhance resin flow. The spiral tube, the foam piece, and the inlet pipe were the major inlet components. The vacuum bag was positioned over the

preform, and bag edges were sealed using sealant tape. Vacuum debulking was performed for 30 min. Resin and hardener were mixed homogeneously and debulked for 10–15 min before injection. During injection, resin first filled the spiral tubes, then spread in a nearly parallel flow front to infuse the preform from top to bottom through the thickness. Once the flow front reached the outlet, and no bubbles were in the tube, both the inlet and outlet were clamped for finishing the infusion (fill) stage. The vacuum infusion protocol was based on thermal analysis of the resin properties (MDSC and rheometry). After the injection was complete (when the entire fabric preform was infused with resin), the laminate was ramped from 20 to 80 °C (at 2 °C/min) on the heated tool plate for 10 h under vacuum. This process advanced the degree of cure and increased green strength, and was followed by free-standing post-cure for 2 h at 110 °C. Figure 2 shows the setup used required for the VI process.

Figure 3 depicts the stages of the process. Once inlet and vent tubes were positioned, the vacuum bag assembly was sealed and closed, the inlet was clamped, and vacuum was applied, a stage referred to as ‘pre-filling’ (Figure 3(a)). The resin/hardener mixing and debulk were also performed at this stage to minimize resin injection time. After pre-filling, the inlet was opened and the resin infiltrated and filled the preform, the “filling stage” (Figure 3(b)). The pressure inside the cavity varied with position and time. Within the impregnated portion of the preform, the resin pressure varied from vacuum (at the flow front) to atmospheric pressure (at the inlet). Once the preform was completely filled, either the inlet was clamped or inlet and vent port directly connected to equilibrate resin pressure within the laminate. In the filling stage, the resin viscosity profile was

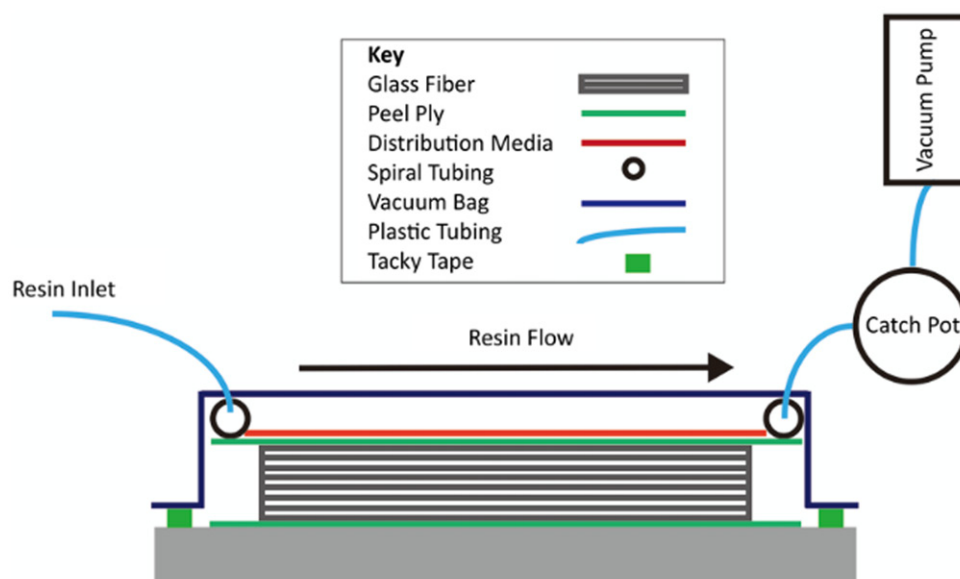


Figure 2. Schematic diagram of a simple VARTM setup for a part made on a flat mold surface.

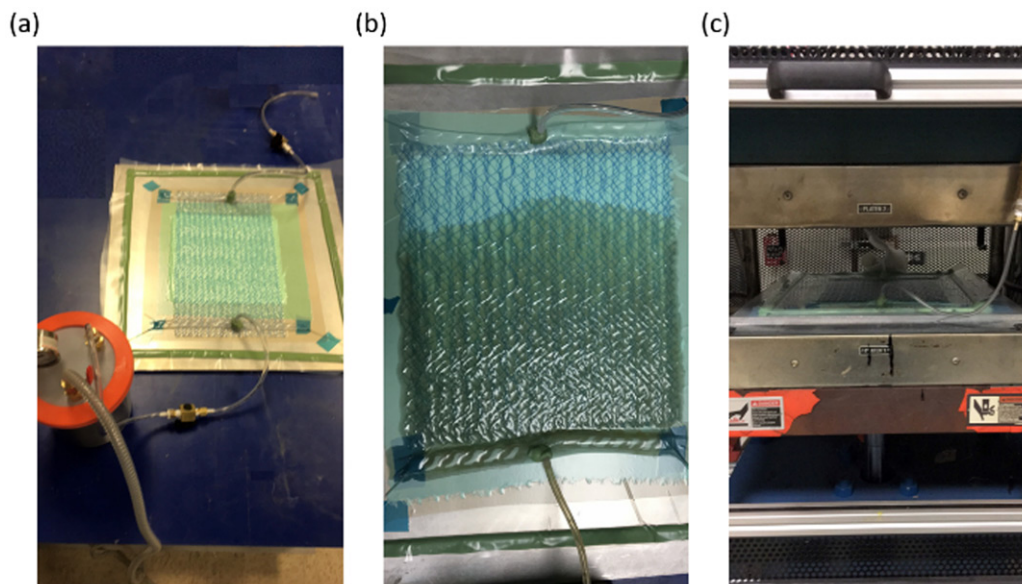


Figure 3. Three stages in the VARTM infusion process: (a) Pre-filling (b) Filling (c) Post-filling Stage.

critical. In our work, the $250 \times 250 \text{ mm}^2$ fabric area was filled in $<5 \text{ min}$ (up to 30–40 min without distribution media) because of the low resin viscosity. The ‘post-filling’ stage (Figure 3(c)) involved removal of excess resin and allowed resin pressure and laminate thickness to equilibrate within the assembly. As excess resin bled through the vent, fiber volume fraction increased, and resin impregnated unsaturated fiber tows or macro-pores.

To ensure acceptable quality, the void contents were measured by image analysis of polished cross-sections. Samples 50 mm long were cut from the part center. Cross-sections were polished to a grit size of 4000. Images of polished sections were acquired at $200\times$ using a digital stereo microscope (Keyence® VHX-6000). Two cross-sections were used to evaluate porosity for each sample. For void content analysis, images were converted to grayscale, and voids were manually selected and filled to distinguish from solid phases. Image analysis code (ImageJ®) was used to “threshold” each image into a binary map of void (black) and solid (white) pixels, and to analyze the resulting areal void ratio.

2.5. Mechanical properties

Mechanical test samples were prepared from the post-cured laminates. Only panels with void contents $<1\%$ were accepted for continued evaluation. All of the test samples were stored in a desiccator prior to testing. Samples (203.2 mm long and 25.4 mm wide) were cut and loaded to failure in tension using a load frame (Instron 5567) in accordance with ASTM D3039. The loading rate was 2 mm/min, eight samples were tested per manufactured panel, and only valid gage section failure cases were chosen. The gauge length was set to 40 mm for all samples.

Compression tests were carried out using a combined loading compression (CLC) fixture (Wyoming Test Fixtures, Salt Lake City, UT) following ASTM D6641. Eight samples (139.7 mm by 12.7 mm) were prepared from each panel with a gauge length of 12.7 mm. Samples were aligned to the test fixture to prevent premature end crushing and limit bending or buckling during testings. The loading rate was 1.3 mm/min to failure.

The flexural properties were determined by three-point bending tests in accordance with ASTM D6272. Four samples were prepared and tested per manufactured panel. The tests were conducted using a load frame (Instron 5567) with a 5000-N load cell. Flexural tests were performed at a strain rate of 0.1 mm/min at room temperature with a load span of 25.5 mm and a support span of 50.7 mm. Beam deflection was measured using a deflectometer (Instron 2601-093).

2.6. Chemical recycling & recovered fiber characterization

Laminates were cut to $120 \times 20 \text{ mm}$ samples and recycled using acid digestion to separate glass fibers from the composites. The standard acid digestion solution consisted of 100 mL glacial acetic acid (Sigma-Aldrich) as a solvent and 10 mL hydrogen peroxide solution (30% (w/w) in H_2O) as the oxidant. An acid digestion process without oxidant was also introduced, since the hydrogen peroxide is a volatile reducing agent and widely considered too hazardous for large-scale industrial use. A three-neck round-bottom flask (1 L) was filled with acid solution, and a composite sample was refluxed at 80 and 110°C . Laminate dissolution in the solvent was determined by observation every 10 min until each

ply could be easily separated. Recycling times were recorded for each acid treatment/temperature condition. Additional hydrogen peroxide solution (30%, 5 mL) was added to the flask every 30 min. Recovered glass fibers were rinsed in water and acetone until no residue was observed. After oven-drying at 120 °C for 30 min, recovered fibers were examined by scanning electron microscopy (SEM, JSM 6610).

2.7. Dissolution comparison study

Cured neat polymer samples were prepared by mixing 0.1 AHEW of curing agent (the Adesso Cleavamine[®] agent shown in Figure 1, and Huntsmann D230) with 0.1 EEW of NPEL 128 epoxy resin (EEW = 184–190 g/eq, Nan Ya Plastics Corporation), degassing the resultant mixture under vacuum, and curing at 80 °C (125 °C for Cleavamine[®] 1) for 2 h followed by 125 °C (150 °C for Cleavamine[®] 1) for 1 h.

The cured neat polymer samples were exposed to three conditions to compare dissolution behavior.

Condition 1: 2 g of glycolic acid and 8 g of water were added to a 250 mL three-necked round bottom flask. The final acetic acid concentration in the solution was 20% (w/w). The flask was heated in an oil bath at 110 °C, then a piece of cured neat polymer sample (1.0 g) was added to the flask. The flask was maintained at 110 °C. The sample was cleaned and dried at select times, and weights were recorded.

Condition 2: 0.5 g of conc. HCl (36.5–38%) and 9.5 g of ethylene glycol were added to a 250 mL three-necked round-bottom flask. The final concentration of HCl in the degradation solution was 1.9% (w/w). The flask was heated in an oil bath at 145 °C, after which a piece of cured sample (1.0 g) was added to the flask. The flask was maintained at 145 °C. The resin sample was cleaned and dried at select times, and weights were recorded.

Condition 3: 3 g of conc. HCl (36.5–38%) and 25 g of ethylene glycol were added to a 250 mL three-necked round-bottom flask. The final concentration of HCl in the degradation solution was 4.0% (w/w). The flask was heated in an oil bath at 145 °C, after which a piece of cured sample (1.0 g) was added to the flask. The flask was maintained at 145 °C. The sample was cleaned and dried at times, and weights were recorded.

3. Results

3.1. Resin properties

The aim of the thermal analysis was to define a cure cycle suitable for composite manufacturing using

the selected resin. TGA tests indicated that the rAFV-2101S resin system began to degrade at ~280 °C, setting not only the maximum temperature for MDSC tests but also a limit for post-cure temperature selection. The dynamic measurements were used to determine the maximum total heat of reaction (H_T) for the resin (368.42 ± 7.57 J/mole). This value was key to determining the degree of cure by isothermal measurements, shown later. The T_g of the cured epoxy was obtained from the inflection point of the last reversible heat flow signal during the ramp cycle ($T_g = 67.4$ °C at a ramp rate of 2 °C/min). The area under the exothermic peak was largely the heat of reaction. The degree of cure, α reached at the end of the isothermal phase was calculated by:

$$\alpha = \frac{H_T - \Delta H_R}{H_T} = 1 - \frac{\Delta H_R}{H_T} \quad (1)$$

The α at three temperatures was determined and values are shown in Figure 4. The symbols represent the different cure time for a given temperature, while the lines are determined from Equation (1) during isothermal cure measurements. The curves show that full cure is approached more rapidly with increasing cure temperature, and that cure at 60 °C may not be sufficient to achieve full cure. The curves in Figure 4 also provide useful guidance for identifying process windows for practical manufacture.

Gelation is defined as the point during the cure cycle when the resin has achieved a flexible but non-flowing molecular structure. In practice, gelation marks the end of the ‘working life’ of the resin and determines the ‘infusion time’ for VI processing. The ‘working life’ or ‘infusion time’ defines the time period for which the resin remains liquid and is able to flow between fibers. Insufficient working time may result in dry fiber areas and compromise the properties of the composite. Gel time and temperature are thus especially critical for thick or large cross-section composites.

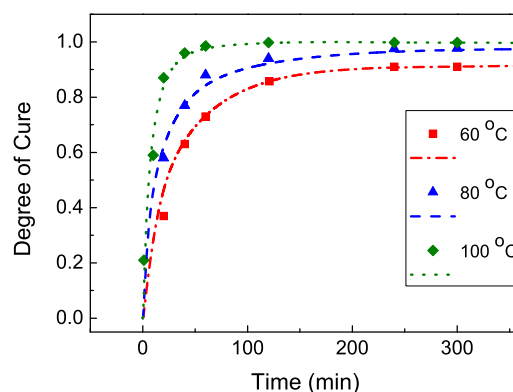


Figure 4. MDSC degree of cure as a function of time at three isothermal cure temperatures.

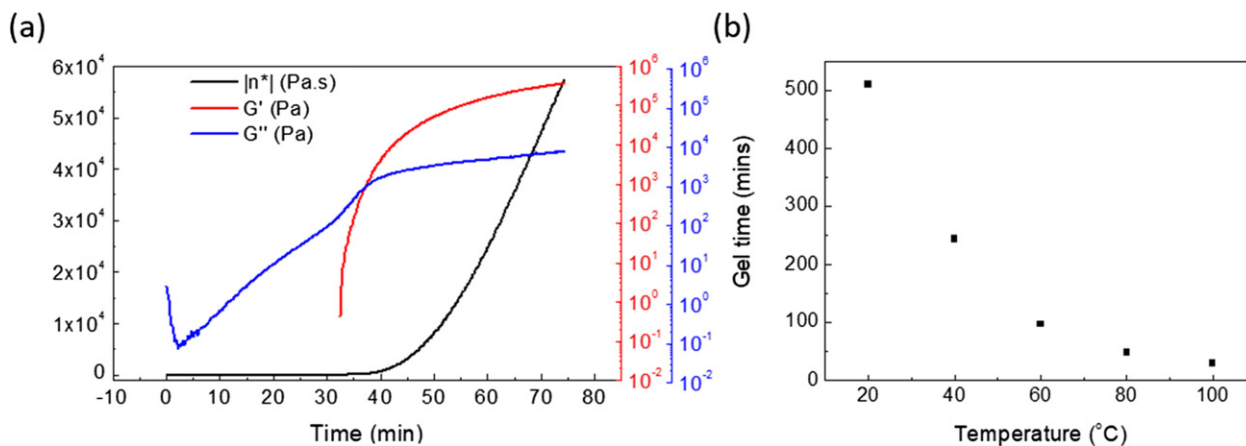


Figure 5. (a) Rheology result for gel time determination of recyclable epoxy resin system. (b) Gel time and temperature as a function of recyclable epoxy resin system.

To estimate resin gel time, isothermal cures were conducted in a rheometer. In rheometric tests, a rotational shear geometry was used to measure the dynamic loss modulus, G'' , and the dynamic storage modulus G' . A sinusoidal oscillation was applied and the resulting stress was measured. In this study, the gel point was defined as the point at which the storage modulus G' exceeded the loss modulus G'' , indicating that the resin transitioned from fluid flow-like behavior to solid elastic behavior. In addition, the viscosity of the resin starts to increase sharply after gelation. In Figure 5(a) and (b), the gel time determined by the intersection between G' and G'' , and the relationship between gel time and isothermal temperature, show that the resin gel time was up to 6.5 h at 20°C , but decreased to less than 40 min when the temperature was 100°C . The parameters determined for cure kinetics and viscosity profile are used to guide the selection of the VI cure cycle.

3.2. Composite characterization

Inspection of polished sections revealed negligible void contents in flat laminates, as shown in images of the 4-ply laminates (Figure 6). Void contents were less than 0.5% with continuous and intimate fiber-resin adhesive contact. The fiber mass ratios of reinforcement and matrix were 0.46 ± 0.02 (2-ply laminates) and 0.49 ± 0.01 (4-ply laminates), respectively.

Because the intended application of the resin system is wind blades, basic mechanical tests were conducted, and the results were compared with properties reported for commercial resins presently used for such applications. Results are summarized in Figure 7, with more details in Table 2. The recyclable composite (Adesso) with the highest T_g , yielded a strength of 88–95% of the value reported for laminates produced with one commercial resin (Hexion), and 100–108% of the value reported for



Figure 6. Polished cross-sections of 4-ply composite laminates under $200\times$ magnification.

laminates produced with another (GURIT). All three products exhibited similar modulus ranges of 20–30 GPa, which is not surprising since modulus is a fiber-dominated property. Also, as we can see in Figure 7, the recyclable composites produced in this study exhibit mechanical strength levels comparable to the two commercial GFRP products presently used in wind blades.

3.3. Composite recycling & recovered fiber surface quality

The viability of deconstructing the cured composites by chemical means was evaluated by measuring dissolution times at atmospheric pressure. In Table 3, the recycling time is presented for laminates of different thickness and for different solvent temperatures. Here, the recycling time of the laminate is defined as the time required for the matrix to fully dissolve in the solvent (determined visually), allowing clean fiber bundles to be fully separated after removal. Without the addition of hydrogen peroxide and at a relatively low temperature, the recycling time for the 2-ply composite sample was less than 1.5 h and less than 2.5 h for the 8-ply laminate. Note that while the number of plies in each laminate was relatively small, the overall thickness was not,

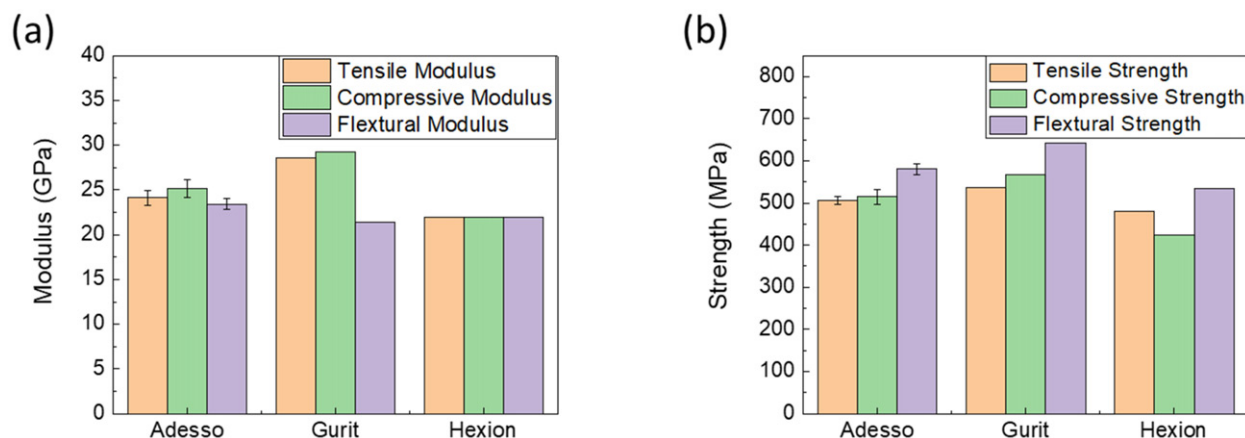


Figure 7. Comparison of mechanical properties with other commercial wind turbine blade resin products in (a) modulus (b) strength.

Table 2. Mechanical and thermal properties comparison.

Company	ADESSO ¹	GURIT ²	HEXION ³	Test Standards for ADESSO resin
T _g (°C)	71.3	69.3	70	DSC (heat rate: 2 °C/min)
Tensile Strength (MPa)	506.2 ± 9.8	536.8	460–500	ASTM D3039
Tensile Modulus (GPa)	24.1 ± 0.8	28.6	20–24	
Compressive Strength (MPa)	514.3 ± 17.3	567.9	410–440	ASTM D6641
Compressive Modulus (GPa)	25.1 ± 1.0	29.2	20–24	
Flexural Strength (MPa)	580.4 ± 12.5	642.2	510–560	Three-point bending ASTM D790
Flexural Modulus (GPa)	23.4 ± 0.6	21.4	20–24	
Cure Cycle (Cure/post-cure)	RT x 10hr + 80°C x 2hr/ 110°C x 2hr	23°C x 24hr/60°C x 15hr	50°C x 16hr	

Note:

¹ADESSO Laminate: 4 plies of Saertex triaxial E-glass, 980 g/m², 3.3 mm thick.

²GURIT Laminate: 4 plies of XE600 biaxial E-glass. (PRIMETM 27 datasheet).

³HEXION Laminate: 16 layers of glass fabric, 8 H satin, 296 g/m², 4 mm thick. (EPIKOTETM RIMR 135 Datasheet).

Table 3. The recycling time under different acid treatment conditions and temperatures with 2,4,8-ply laminates.

Acid Treatment/Temperature	2 plies (~1.7 mm)	4 plies (~3.3 mm)	8 plies (~6.7 mm)
Aceric acid/H ₂ O ₂ , 110 °C	30 mins	50 mins	80 mins
Aceric acid, 110 °C	50 mins	70 mins	100 mins
Aceric acid, 80 °C	80 mins	100 mins	130 mins

Note: All experiments processed under atmospheric pressure.

because of the high areal weight of the NCF. Recycling temperatures were modest, and times were generally under 2 h, without application of super-ambient pressure.

Figure 8(a) shows the recycled GF and the parent laminate at different stages of dissolution. The center image in Figure 8(a) shows the effects of partial immersion in the digestion solution, while the image at right shows the recovered fibers. Note that the fiber architecture of the NCF is partially preserved, indicating the possibility of retaining fabric architecture after separation from the matrix. Figure 8(b) shows the reclaimed matrix residue obtained after the neutralization reaction, which manifests as a powdery substance comprised of molecular fragments of the parent polymer, as yet unidentified. The image demonstrates that complete dissolution of the matrix can be achieved via acid digestion under mild conditions.

Figure 8(c) compares the post-digestion appearance a laminate produced using the recyclable epoxy resin (on the left) with a comparable laminate produced with a commercial amine-cured epoxy (bifunctional epoxy monomer (diglycidyl ether of bisphenol A (DGEBA), Araldite GY 6010, Huntsman) and diamine 3,3'-diaminodiphenylsulfone curing agent (3,3'-DDS, Aradur[®] 9719-1, Huntsman) (on the right). Samples of each type of laminate were partially immersed in the same digestion solution for identical times. The image demonstrates that complete dissolution of the recyclable epoxy matrix can be achieved in moderate conditions (acetic acid/H₂O₂ treatment at 110 °C for 30 mins). However, the conventional amine-cured epoxy laminate shows only slight matrix dissolution after 24 h treatment.

The quality of glass fibers recovered after matrix digestion was examined to ascertain surface quality

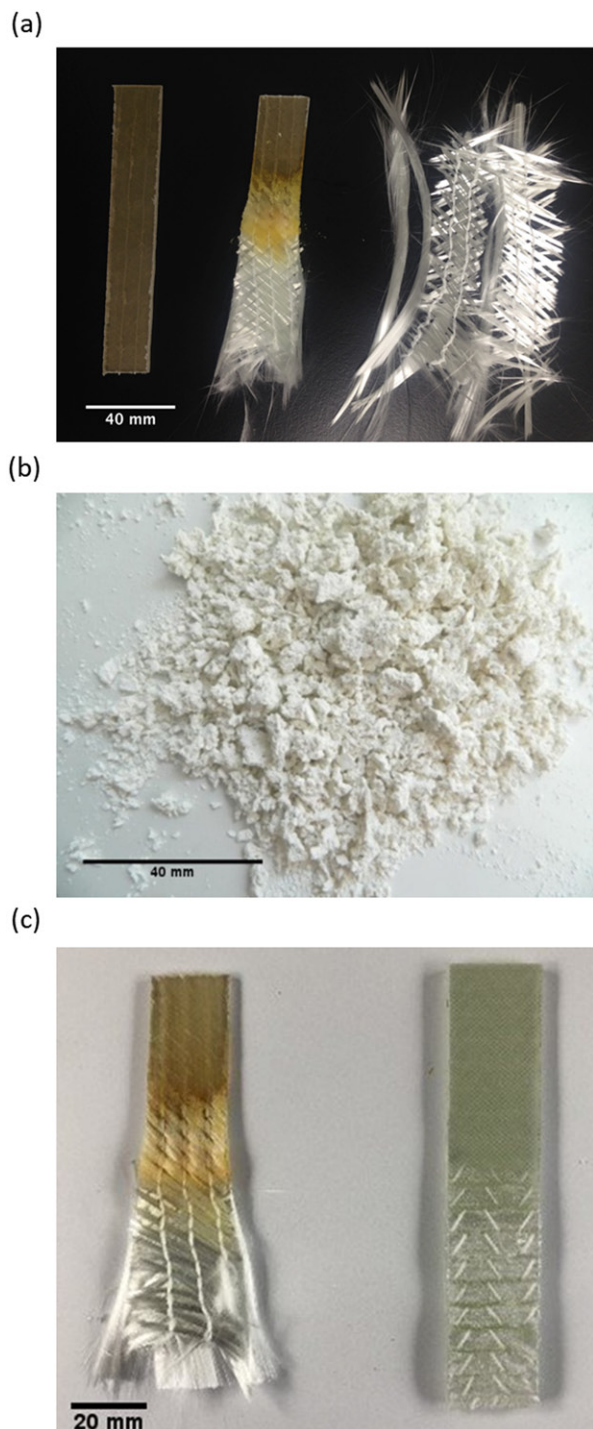


Figure 8. (a) Recovered glass fibers after Acid-digestion treatment, (b) reclaimed resin powder after recycling and (c) recyclability comparison with other commercial epoxy system.

and detect any matrix residue on fiber surfaces. Figure 9(a) shows virgin glass fibers compared with glass fibers recovered from a typical acid digestion treatment at 110 °C (Figure 9(b)). The fiber surfaces show no evidence of change after acid digestion at 110 °C or at lower temperature (80 °C) and in milder conditions (without using hydrogen peroxide). The recovered fiber surface quality is identical to the surface quality of virgin glass fibers, and no surface defects or residues are evident. The

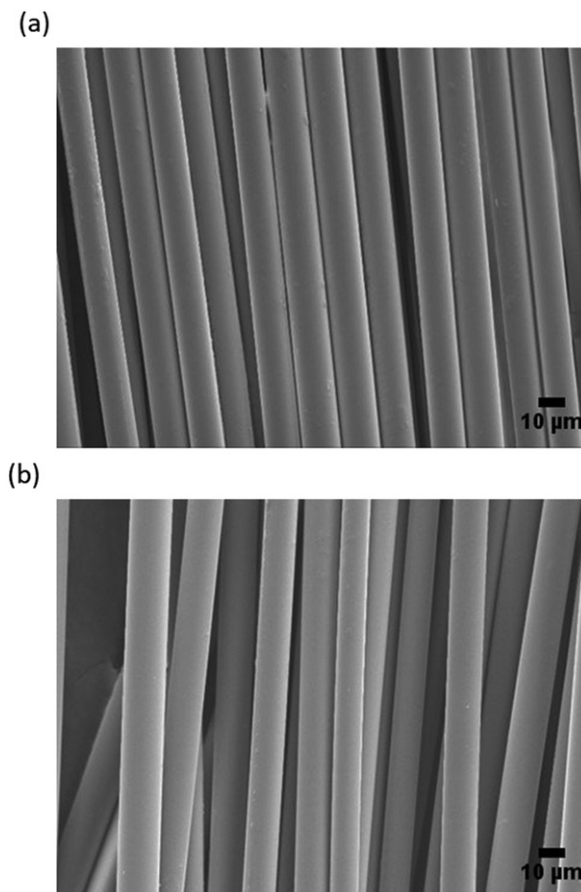


Figure 9. Virgin glass fiber and recovered fiber surfaces after different temperature treatments: (a) Virgin glass fiber; (b) Acetic acid, 110 °C.

diameters of recovered fibers are slightly less (roughly 13 μm versus 16 μm) than those of virgin fibers perhaps due to the removal of the sizing during acid digestion, which may lead to weaker adhesion to the polymer matrix in subsequent re-use applications.

3.4. Reclaimed resin properties

After separating fibers from the matrix, matrix residue powders (recyclate) were blended with neat resin (from 5 wt% up to 20 wt%, without any further chemical modification), then combined with fiber reinforcement by resin infusion and cured. The flexural properties and glass transition temperature (T_g) (determined by DSC) of the resultant blended polymers were then compared, to determine the dependence on recyclate fraction, as shown in Figure 10. When residue powder content of up to 5% was added, the value of strength and T_g were similar to the control (virgin polymer), indicating full retention of properties.

Thermal properties of reclaimed resin were also evaluated, and dynamic mechanical analysis (DMA) was used to measure T_g from the storage modulus (E'), as well as from the tangent of the loss angle

(δ). Figure 11 shows the change in the storage modulus E' and $\tan\delta$ for selected temperature ramp procedures ($5^\circ\text{C}/\text{min}$, ramp from 20 to 200°C). The values from DMA analysis are also presented in Table 4. A significant decrease in the storage modulus was noted when the reclaimed resin content in the polymer matrix exceeded 10%. At 25°C , the value of E' decreased by 43% with a 20% share of the filler in relation to the (virgin) neat polymer. The results indicate that additions of 10–20% recycle caused both the strength and the T_g to decrease in proportion to the percentages of recycle added. Thus, the recycle effectively acted more as a filler than as a molecular component of the cross-linked polymer network.

3.5. Dissolution

To understand the effects of different types of formal/ketal bonds on the degradation potential in cured epoxy, a series of comparison studies were conducted. A summary of the results is shown in Figure 12. All cured samples were prepared from an EEW:AHEW = 1:1 mixture of a selected curing agent and epoxy resin (NPEL128) to assure equivalent degrees of crosslinking in the cured polymer. The epoxy resin sample cured with Cleavamine[®]

curing agent 3, which contains a ketal bond linking the two aliphatic amino groups, showed 100% dissolution in 20% acetic acid aqueous solution within 1 hour at 110°C (black filled rectangles in Figure 12). Likewise, the same samples showed complete dissolution in 1.9% HCl aqueous solution containing a common organic solvent, ethylene glycol, within 1.5 h at 145°C (red filled circles in Figure 12). In contrast, its equivalent, cured with Cleavamine[®] 2, required a higher concentration of 4% HCl in the aqueous ethylene glycol system, and a longer dissolution period, up to 20 h for degradation completion heated at 145°C (blue filled triangles in Figure 12). The Cleavamine[®] 2 contains a formal bond linking the two aliphatic amino groups.

Under the same degradation conditions, epoxy resin samples cured with a commercial cure agent

Table 4. Summarising the glass transition temperature values and storage modulus values of the different wt% reclaimed Epoxy/GF composites.

Reclaimed resin content (wt%)	T_g ($^\circ\text{C}$)		
	E' Onset	$\tan\delta$	E' at 25°C (MPa)
0	68.0	74.6	10451
5	67.1	72.8	10094
10	61.4	69.1	9383
20	53.1	63.9	6034

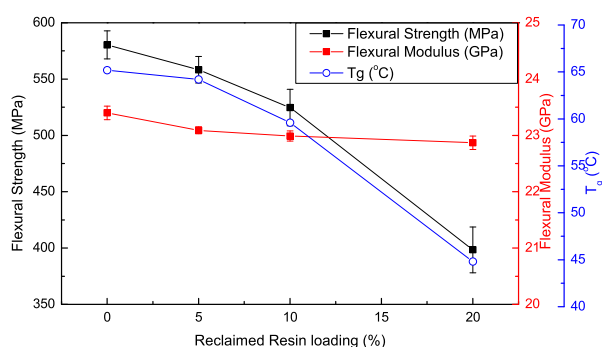


Figure 10. Flexural strength, flexural modulus and glass transition temperature (T_g) of neat polymer blended with reclaimed recycle (powder), as a function of recycle loading.

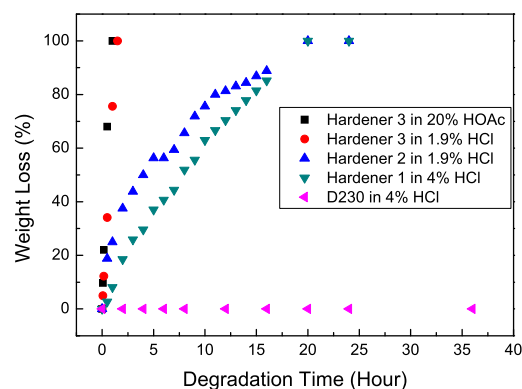


Figure 12. Degradability of different types of formal/ketal bonds hardeners in cured epoxy.

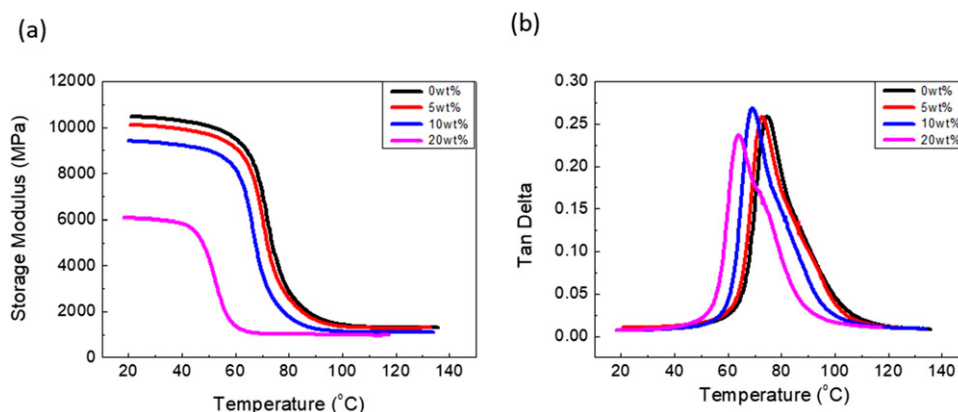


Figure 11. The (a) storage modulus (E') and (b) $\tan\delta$ values from DMA to determine the glass transition temperature.

(Huntsman D230) did not exhibit any degradation over a period of 24 h (purple filled triangles in Figure 12). Note that the dissolution of the epoxy sample cured with Cleavamine[®] 1, which contains a formal bond directly linking two phenyl rings comprising amino groups, was achieved in less than 20 h in 1.9% HCl aqueous solution at 145 °C (dark cyan filled down triangles in Figure 11). We conclude that among the three Cleavamine[®] curing agents, the dissolution potential is greatest in those with the ketal bond, followed by those with the formal bond, besides, the phenyl formal bond dissolution time is less than the aliphatic formal bond.

4. Conclusions

We have demonstrated the feasibility of using recyclable epoxy resin in VI processing of composites. In addition, we have demonstrated the ability to subsequently separate fibers from matrix, while recovering matrix components that are potentially eligible for re-use. The separation process was conducted by acid digestion *under mild conditions* (atmospheric pressure and without using strong oxidizer), and affords the *opportunity to recover and re-use both high-value fibers as well as useful parts of matrix molecules*. The recovered glass fibers retained near-virgin fiber surface quality, while the recovered matrix residue was suitable for blending with virgin epoxy for re-use in second-life applications. The thermal and mechanical properties of the recyclable polymer showed performance characteristics comparable to typical non-recyclable infusion resins, allowing direct substitution for commercial resins without sacrificing performance. Also, the resin chemistry and degradability mechanism of recycled resin had been included.

Despite these promising results, challenges remain. First, the key component of the digestive solution, H₂O₂, is both costly and explosive, and in all likelihood, it cannot be safely deployed on an industrial scale. Thus, this reagent must be eliminated from the digestion process and replaced with a safer surrogate. Doing so will increase the value of dissolution products, reduce intrinsic hazard, and increase the net value of recovered FRP components. Secondly, we have demonstrated matrix digestion only on small laminates, and the reaction kinetics must be proven on much larger parts, often with protective coatings, attached core materials, and fasteners.

We have demonstrated a pathway to a closed-loop recycling process for thermoset composites. Future efforts must focus on developing more cost-effective and safer recycling routes for both reclaimed resin and recycled fibers. In addition, efforts

must focus on restoring the adhesion properties of recovered fibers to levels comparable to virgin fibers. Finally, the prospect of recycling not only fibers but polymer matrix would enhance sustainability of future composite products, but not those composites presently in use. A scalable solution to that problem most likely will require a clever chemical solution, as yet unknown.

Acknowledgments

Support from the M.C. Gill Composites Center is gratefully acknowledged. The SEM images presented in this article were acquired at the Center for Electron Microscopy and Microanalysis at the University of Southern California. Adesso Advanced Materials Corporation generously donated the epoxy resins and curing agents used in this study. The SEM images presented in this article were acquired at the Center for Electron Microscopy and Microanalysis at the University of Southern California.

Disclosure statement

No potential conflict of interest was reported by the authors.

ORCID

Ming-Sung Wu  <http://orcid.org/0000-0001-8820-4734>

References

- [1] AWEA U.S. Wind Industry Annual Market Report, American wind energy association, 2018.
- [2] Global Wind Report 2015. Global Wind Energy Council, 2015.
- [3] Flizikowski J, Bielinski K. Technology and energy sources monitoring: control, efficiency and optimization. IGI Global. 2013. ISBN 9781466626645.
- [4] Wu M-S, Centea T, Nutt SR. Compression molding of reused in-progress waste effects of material and process factors. J Adv Manufact Polymer Compos Sci. 2018;4:1–12.
- [5] Kratz J, Low YS, Fox B. Resource-friendly carbon fiber composites: combining production waste with virgin feedstock. J Adv Manufact Polymer Compos Sci. 2017;3:121–129.
- [6] Miyake T, Imaeda S. A dry aligning method of discontinuous carbon fibers and improvement of mechanical properties of discontinuous fiber composites. J Adv Manufact Polymer Compos Sci. 2016;2:117–123.
- [7] Khanam PN, AlMaadeed MAA. Processing and characterization of polyethylene-based composites. J Adv Manufact Polymer Compos Sci. 2015;1: 63–79.
- [8] Gong G, Olofsson K, Nyström B, et al. Experimental verification of Re-Fib method for recycling fibres from composites. J Adv Manufact Polymer Compos Sci. 2016;2:27–33.
- [9] Jin BC, Li X, Jain A, et al. Optimization of microstructure and mechanical properties of composite

- oriented strand board from reused prepreg. *J Compos Struct.* 2017;174:389–398.
- [10] Jin BC, Li X, Jain A, et al. Prediction of stiffness of reused carbon fiber/epoxy composite oriented strand board using finite element methods. *Recycl Mater Struct Soc Advance Mater Process Eng J.* 2017;53:32–39.
 - [11] Jin BC, Li X, Jain A, et al. Development of a finite element model for reused carbon fiber epoxy composite oriented strand board. Society for the Advancement of Material and Process Engineering Technical Conference (SAMPE Tech), LB15-0347, Long Beach, 2016.
 - [12] Jin BC, Li X, Wu M-S, et al. Nondestructive testing and evaluation of conventional and reused carbon fiber epoxy composites using ultrasonic and stitched micro-CT. SAMPE Tech. LB15-0342, Long Beach, 2016.
 - [13] Ma Y, Kim D, Nutt SR. Chemical treatment for dissolution of amine-cured epoxies at atmospheric pressure. *Polym Degrad Stab.* 2017;146:240–249.
 - [14] Wu M-S, Centea T, Nutt SR. Process optimization for compression molding of reused prepreg scrap. Proceedings of the 29th Tech Conf ASC 8-11 September San Diego, CA, USA, Dayton, OH, USA. ASC Composites, 2014.
 - [15] Pimenta S, Pinho ST. Recycling carbon fiber reinforced polymers for structural applications: Technology review and market outlook. *Waste Manage.* 2011;31:378–392.
 - [16] Pimenta S, Pinho ST. The effect of recycling on the mechanical response of carbon fibers and their composites. *Composite Structures.* 2012;94:3669–3684.
 - [17] LeBlanc D, Landry B, Levy A, et al. Compression molding of complex parts using randomly-oriented strands thermoplastic composites. Proceedings of the SAMPE Tech. Conf. 2–4 June Seattle, USA, Covina, CA: SAMPE, 2014.
 - [18] Lee H, Neville K. Handbook of epoxy resins. New York: McGraw-Hill, 1967.
 - [19] Hawkins WL. Polymer degradation and stabilization. Berlin: Springer-Verlag, 1984.
 - [20] Jacob A. Composites can be recycled. *Reinf Plast.* 2011;55:45–46.
 - [21] Palmer J, Ghita OR, Savage L, et al. Successful closed-loop recycling of thermoset composites. *Compos Part A Appl Sci Manuf.* 2009;40:490–498.
 - [22] Pickering SJ. Recycling technologies for thermoset composite materials – current status. *Compos Part A.* 2006;37:1206–1215.
 - [23] Schinner G, Brandt J, Richter H. Recycling carbon-fiber-reinforced thermoplastic composites. *J Thermoplast Compos Mater.* 1996;9:239–245.
 - [24] Kouparitsas CE, Kartali CN, Varelidis PC, et al. Recycling of the fibrous fraction of reinforced thermoset composites. *Polym Compos.* 2002;23:682–699.
 - [25] Takahashi J, Matsutsuka N, Okazumi T, et al. Mechanical properties of recycled CFRP by injection molding method. Proceedings of the 16th International Conference on Composite Materials 8–13 July 2007, Kyoto, Japan.
 - [26] Ogi K, Nishikawa T, Okano Y, et al. Mechanical properties of ABS resin reinforced with recycled CFRP. *Adv Compos Mater.* 2007;16:181–194.
 - [27] Palmer J, Savage L, Ghita OR, et al. Sheet molding compound (SMC) from carbon fibers recycle. *Compos Part A.* 2010;41:1232–1237.
 - [28] Ushikoshi K, Komatsu N, Sugino M. Recycling of CFRP by pyrolysis method. *J Soc Mater Sci Japan.* 1995;44:428.
 - [29] Zheng Y, Shen Z, Ma S, et al. A novel approach to recycling of glass fibers non-metal materials of waste printed circuit boards. *J Hazard Mater.* 2009;170:978–982.
 - [30] Gosau JM, Tyler FW, Allred RE. Carbon fiber reclamation from state-of-art 2nd generation aircraft composites. Proceedings of the International SAMPE Symposium and Exhibition, May 18–21, 2009, Baltimore, MD, USA.
 - [31] Lester E, Kingman S, Wong KH, et al. Microwave heating as a means for carbon fibers recovery from polymer composites: a technical feasibility study. *Mater Res Bull.* 2004;39:1549–1556.
 - [32] Akesson D, Foltynowicz Z, Christeen J, et al. Microwave pyrolysis as a method of recycling glass fibers from used blades of wind turbines. *J Reinf Plast Compos.* 2012;31:1136–1142.
 - [33] Nahil MA, Williams PT. Recycling of carbon fiber reinforced polymeric waste for the production of activated carbon fibers. *J Anal Appl Pyrol.* 2011;91:67–75.
 - [34] Morin C, Loppinet-Serani A, Cansell F, et al. Near- and supercritical solvolysis of carbon fiber reinforced polymers (CFRPs) for recycling carbon fibers as a valuable resource: state of the art. *J Supercrit Fluids.* 2012;66:232–240.
 - [35] Feraboli P, Kawakami H, Wade B, et al. Recyclability and reutilization of carbon fiber fabric/epoxy composites. *J Compos Mater.* 2012;46:1459–1473.
 - [36] Li J, Xu PL, Zhu YK, et al. A promising strategy for chemical recycling of carbon fiber/thermoset composites: self-accelerating decomposition in a mild oxidative system. *Green Chem.* 2012;14:3260–3263.
 - [37] Xu PL, Li J, Ding JP. Chemical recycling of carbon fiber/epoxy composites in a mixed solution of peroxide hydrogen and N, N-dimethylformamide. *Compos Sci Technol.* 2013;82:54–59.
 - [38] Liu Y, Liu J, Jiang Z, et al. Chemical recycling of carbon fiber reinforced epoxy resin composites in subcritical water: synergistic effect of phenol and KOH on the decomposition efficiency. *Polym Degrad Stab.* 2012;97:214–220.
 - [39] Oliveux G, Dandy LO, Leeke GA. Degradation of a model epoxy resin by solvolysis routes. *Polym Degrad Stab.* 2015;118:96–103.
 - [40] Okajima I, Hiramatsu M, Shimamura Y, et al. Chemical recycling of carbon fiber reinforced plastic using supercritical methanol. *J Supercrit Fluids.* 2014;91:68–76.
 - [41] Jain A, Jin BC, Nutt SR. Mean-field homogenization methods for strand composites. *J Comp B.* 2017;124:31–39.
 - [42] Ma Y, Kim D, Nutt SR. A parametric study of the recyclability of carbon fiber reinforced polymers. Proceedings of the 2016 Society for the Advancement of Material and Process Engineering (SAMPE) Technical Conference, 2016. Long Beach, CA, May 23–26.

- [43] Navarro CA, Kedzie EA, Ma Y, et al. Mechanism and catalysis of oxidative degradation of fiber-reinforced epoxy composites. *Top Catal.* 2018;61:704–709.
- [44] Dang W, Kubouchi M, Sembokuya H, et al. Chemical recycling of glass fiber reinforced epoxy resin cured with amine using nitric acid. *Polymer* 2005;46:1905–1912.
- [45] Wong KH, Pickering SJ, Rudd CD. Recycled carbon fibre reinforced polymer composite for electromagnetic interference shielding. *Compos Part A.* 2010;41:693–702.
- [46] Wong KH, Mohammed DS, Pickering SJ, et al. Effect of coupling agents on reinforcing potential of recycled carbon fibre for polypropylene composite. *Compos Sci Technol.* 2012;72:835–844.
- [47] Akonda MH, Lawrence CA, Weager BM. Recycled carbon fibre-reinforced polypropylene thermoplastic composites. *Compos Part A.* 2012;43:79–86.
- [48] Meredith J, Cozien-Cazuc S, Collings E, et al. Recycled carbon fibre for high performance energy absorption. *Compos Sci Technol.* 2012;72:688–695.
- [49] Stoeffler K, Andjelic S, Legros N, et al. Polyethylene sulphide (PPS) composites reinforced with recycled carbon fiber. *Compos Sci Technol.* 2013;84:65–71.
- [50] Teenkamer DA, Sullivan JL. On the recyclability of a cyclic thermoplastic composite material. *Compos Part B.* 1998;29:745–752.
- [51] Pastine S, Liang B, Qin B. Novel agents for reworkable epoxy resins. WO 2012/071896, 2013.
- [52] Liang B, Qin B, Pastine S, et al. Reinforced composite and method for recycling the same. U.S. Patent 9598551, 2017.
- [53] Qin B, Li X, Liang B. Novel Curing agents and degradable polymers and composites based thereon. WO 2014/169847, 2014.
- [54] Watson ES, O'Neill MJ. Differential Microcalorimeter. Patent 3,263,484. 2 August, 1966.
- [55] Thomas LC. Modulated DSC Paper#1 Why Modulated DSC? An overview and summary of advantages and disadvantages relative to traditional DSC. TA Instruments Technol. Pap. 2005, TP, 006.
- [56] Wunderlich B. Quasi-Isothermal Temperature-Modulated Differential Scanning Calorimetry (TMDSC) for the separation of reversible and irreversible thermodynamic changes in glass transition and melting ranges of flexible macromolecules. *Pure Appl Chem.* 2009;81:1931–1952.
- [57] Simon SL. Temperature-modulated differential scanning calorimetry: theory and application. *Thermochim Acta.* 2001;374:55–71.